Arany, L., Bhattacharya, S., Adhikari, S., Hogan, S. J., & Macdonald, J. H. G. (2015). An analytical model to predict the natural frequency of offshore wind turbines on three-spring flexible foundations using two different beam models. *Soil Dynamics and Earthquake Engineering*, *74*, 40 - 45. https://doi.org/10.1016/j.soildyn.2015.03.007

An analytical model to predict the natural frequency of offshore wind turbines on three-spring flexible foundations using two different beam models

L. Arany[1], S. Bhattacharya[2], S. Adhikari[3], S. J. Hogan[4], J. Macdonald[5]

[1,4,5] University of Bristol,

[2] University of Surrey,

[3] Swansea University, UK,

Corresponding author:

Professor Subhamoy Bhattacharya

Email: S.Bhattacharya@surrey.ac.uk

Phone number: +44 (0) 1483 68 9534

ABSTRACT: In this study an analytical model of offshore wind turbines (OWTs) supported on flexible foundation is presented to provide a fast and reasonably accurate natural frequency estimation suitable for preliminary design or verification of Finite Element calculations. Previous research modelled the problem using Euler-Bernoulli beam model where the foundation is represented by two springs (lateral and rotational). In contrast, this study improves on previous efforts by incorporating a cross-coupling stiffness thereby modelling the foundation using three springs. Furthermore, this study also derives the natural frequency using Timoshenko beam model by including rotary inertia and shear deformation. The results of the proposed model are also compared with measured values of the natural frequency of four OWTs obtained from literature. The results show that the Timoshenko beam model does not improve the results significantly and the slender beam assumption may be sufficient. The cross-coupling spring term has a significant effect on the natural frequency therefore needs to be included in the analysis. The model predicts the natural frequency of existing turbines with reasonable accuracy.

Keywords: Beam theory, offshore wind turbine, soil-structure interaction, natural frequency, Timoshenko, Euler-Bernoulli, monopile foundation

1. Introduction

In order to ensure the optimum performance throughout the design life, predicting the long term behaviour of offshore wind turbines (OWTs) is essential. However, data are scarce on the long term performance of these complex mechanical systems consisting of the foundation, the substructure, the tower and the rotor-nacelle assembly. The loading of OWTs is complex due to a combination of static, cyclic and dynamic loads [1]. OWTs must be designed to avoid the frequency range of the forcing (wind turbulence and water wave spectra) and also the rotational frequency (1P) and the blade passing frequency (3P for a three-bladed turbine) ranges of the turbine. The importance of dynamics for offshore wind turbines is well established in the literature ([1]–[5]), and further explanation is omitted here. It is well known from literature that repeated cyclic or dynamic loads (further details can be found in [12] [13] [14]) on a soil cause a change in the properties which in turn can alter the stiffness of the foundation ([2], [6], [7]). A wind turbine structure derives its stiffness from the support i.e. the foundation and any change in the stiffness may shift the natural frequency closer to the forcing frequencies. This issue is particularly problematic to the soft-stiff structure (natural frequency between 1P and 3P frequency) as any increase or decrease in the natural frequency will impinge on the forcing frequencies and may lead to unplanned resonance and increased fatigue damage. This may lead to loss of years of service, which is to be avoided.

Difference between design and measured natural frequency is reported in the literature. Two examples are considered here: (a) *Walney 1 Wind farm*: The actual natural frequency was 6-7% higher than the estimated for a Siemens SWT-3.6-107 turbine at the Walney 1 site, see Kallehave and Thilsted [9]; (b) *Twisted jacket at Hornsea Site*: Difference between the design and measured frequency was observed in the case of the Hornsea Met Mast supported on a 'Twisted Jacket' foundation [8]. In this demonstration project it was found that the foundation was stiffer than expected and the initial measured frequency was 1.28-1.32Hz as opposed to the design frequency of 1Hz. Furthermore, after three months, the natural frequency shifted to 1.13-1.15Hz, likely due to softening of the soil. These cases clearly highlight the importance of prediction of the natural frequency.

The aim of this work is to provide an analytical estimation for the natural frequency of monopile supported offshore wind turbines where the foundation is modelled using three springs: (a) Lateral spring (K_L); (b) Rotational spring (K_R); (c) A cross coupling spring (K_{LR}) which is in contrast to the uncoupled springs model ([1], [3], [9], [10]). Furthermore, present study also extends the analysis by incorporating the Timoshenko beam model ([11], [12]) which also accounts for rotary inertia and shear deformation.

2. Structural model of the offshore wind turbine

The structural model used in this paper is shown in Fig 1. The foundation is represented by three springs: lateral K_L, rotational K_R and cross K_{LR} stiffness. The tower is idealised by equivalent bending stiffness and mass per length following [9], [13] and is modelled by two different partial differential equations using Euler-Bernoulli beam model, and Timoshenko beam model. The later accounts for shear deformation and the effect of rotational inertia. The nacelle and rotor assembly is modelled as a top head mass with mass moment of inertia.

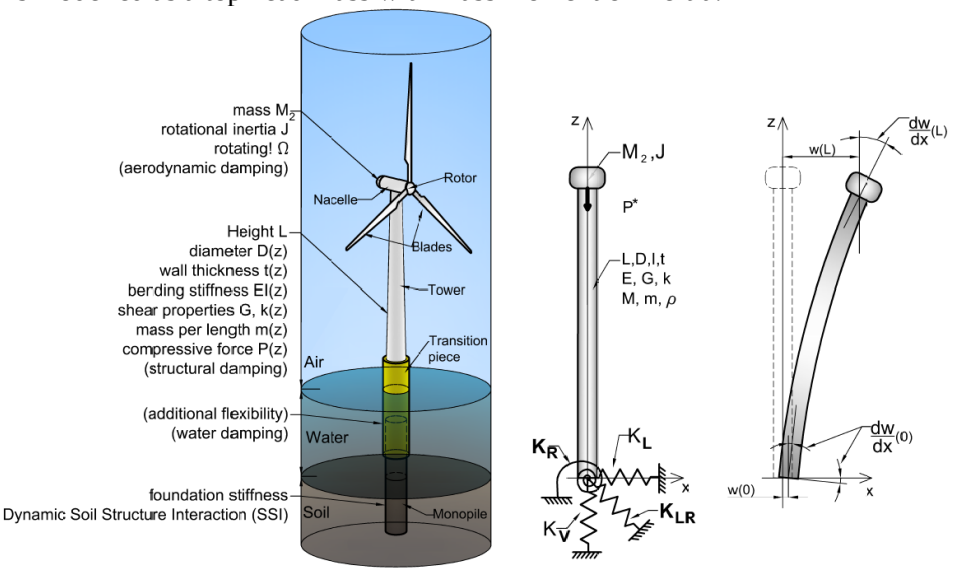

Figure 1 – Mechanical model of a wind turbine.

Table 1 – Non-dimensional groups: definitions and practical range

Dimensionless group	Formula	Typical values
Non-dimensional lateral stiffness	$\eta_L = K_L L^3/EI$	2500 – 12000
Non-dimensional rotational stiffness	$\eta_R = K_R L/EI$	25 – 80
Non-dimensional cross stiffness	$\eta_{LR} = K_{LR} L^2/EI$	(-515) – (-60)
Non-dimensional axial force	$\nu = P^* L^2/EI$	0.005 – 0.1
Mass ratio	$\alpha = M_2/M_3$	0.75 – 1.2
Non-dimensional rotary inertia	$\beta = J/mL^2$	*
Non-dimensional shear parameter	$\gamma = E/Gk$	~4.5 (for steel tubular towers)
Non-dimensional radius of gyration	$\mu = r/L$	0.008 – 0.025
Frequency scaling parameter	$c_0 = \sqrt{EI/M_3 L^3}$	~1-5
Non-dimensional rotational frequency	$\Omega_k = \omega_k/c_0 = \omega_k\sqrt{EI/M_3 L^3}$	-

K_L, K_R, K_{LR} are the lateral, rotational and cross stiffness of the foundation, respectively; EI is the equivalent bending; L is the height of the tower; P^* is the modified axial force (see Equation 3), M_2 is the top head mass; M_3 is the mass of the tower; J is the rotary inertia of the top mass; m is the equivalent mass per unit length of the tower; $r = \sqrt{I/A}$ is the radius of gyration of the tower, ω_k is the kth natural frequency.
**The rotary inertia is taken to be zero for all wind turbines considered as information is not available in the referenced literature.*

2.1 Foundation model

In Fig 1 the foundation is represented by four springs, a lateral K_L, a rotational K_R, a cross coupling K_{LR} and also a vertical spring, which is neglected because the structure is very stiff vertically. The method of Gazetas [14] can be used for the estimation of the stiffness of slender piles (recommended in Eurocode 8, Part 5 [15]), however, it is not validated for very large diameter piles. In the absence of directly measured values of stiffness, the Finite Element (FE) approach may produce better results (see e.g. Lesny et al. [16]). The three spring model can be written with a stiffness matrix as the following:

$$\begin{bmatrix} F_x \\ M_y \end{bmatrix} = \begin{bmatrix} K_L & K_{LR} \\ K_{LR} & K_R \end{bmatrix} \begin{bmatrix} w \\ w' \end{bmatrix} \tag{1}$$

where F_x is the lateral force, M_y is the fore-aft moment, w is the displacement and $w' = \partial w/\partial z$ is the slope.

2.2 Model of the rotor-nacelle assembly

The rotor-nacelle assembly is modelled as a top head mass M_2 with mass moment of inertia J, as shown in Fig 1. These parameters are used in formulating the end boundary conditions of the PDEs of the motion of the tower in Sections 2.3.1 and 2.3.2. In addition, the mass M_2 exerts a downwards pointing force P due to gravity, and the self-weight of the structure also acts on the sectons below. The total vertical force is:

$$P = -M_2 g - mg(L - z) \tag{2}$$

where m is the average mass per length of the tower, L is the height of the tower. An approximate expression for a constant force P^* is followed here as given in Adhikari and Bhattacharya [9]:

$$P^* = -M_{corr} g = -(M_2 + C_M M_3) g \tag{3}$$

where M_{corr} is the corrected mass, M_3 is the mass of the tower. The mass correction factor is $C_M = 33/140 \approx 0.24$ for a cantilever beam, and using the non-dimensional numbers from Table 1, for flexible foundations ([9]):

$$C_M = \frac{3}{140} \cdot \frac{11\eta_R^2\eta_L^2 + 77\eta_L^2\eta_R + 105\eta_R^2\eta_L + 140\eta_L^2 + 420\eta_L\eta_R + 420\eta_R^2}{9\eta_R^2 + 6\eta_R^2\eta_L + 18\eta_R\eta_L + \eta_R^2\eta_L^2 + 6\eta_L^2\eta_R + 9\eta_L^2} \tag{4}$$

2.3 Modelling the tower

For slender beams Euler-Bernoulli beam model can be used, for more stocky beams Timoshenko beam theory is necessary. The two models are compared here and the tapered tower is replaced by an equivalent bending stiffness assuming constant wall thickness. The non-dimensional numbers defined in Table 1 are used in this derivation. The Euler-Bernoulli beam derivations can be found in [9], [10] and therefore only the Timoshenko beam model is derived. The equations of motion for Timoshenko beams were derived by Timoshenko in his papers [11] and [12]:

$$-GkA\left(\frac{\partial^2 w(z,t)}{\partial z^2} - \frac{\partial \Theta(z,t)}{\partial z}\right) + \rho A \frac{\partial^2 w(z,t)}{\partial t^2} = p(z,t) \quad \text{and} \quad EI\frac{\partial^2 \Theta(z,t)}{\partial z^2} + GkA\left(\frac{\partial^2 w(z,t)}{\partial z^2} - \frac{\partial \Theta(z,t)}{\partial z}\right) - I\rho\frac{\partial^2 \Theta(z,t)}{\partial t^2} = 0 \tag{5}$$

where $w(z,t)$ is the transversal displacement; ρ is the density of tower material; A is the cross section area; k is the Timoshenko shear coefficient; G is the shear modulus; $p(z,t)$ is the external force; E is Young's modulus; I is the area moment of inertia of the cross section and $\Theta(z,t)$ is the angle due to pure bending. These two equations can be transformed into one as shown in [17]. Looking at free vibrations, the single equation becomes:

$$EI\frac{\partial^4 w(z,t)}{\partial z^4} - \left(\frac{\rho EI}{Gk} + \rho I\right)\frac{\partial^4 w(z,t)}{\partial z^2 \partial t^2} + \frac{\rho^2 I}{Gk}\frac{\partial^4 w(z,t)}{\partial t^4} + \rho A\frac{\partial^2 w(z,t)}{\partial t^2} = 0 \tag{6}$$

Using separation of variables and assuming a harmonic solution, including the axial force P^* and using the dimensionless axial coordinate $\xi = z/L$:

$$W^{IV} + \left(\frac{P^* L^2}{EI} + \frac{\omega^2 \rho I L^2}{EI} + \frac{\omega^2 \rho L^2}{Gk}\right)W'' + \left(\frac{\omega^4 \rho^2 I L^4}{EIGk} - \frac{\omega^2 \rho A L^4}{EI}\right)W = 0 \tag{7}$$

Few points may be noted: If shear deformation is to be excluded from the equation, it can be done by letting $G \to \infty$. If rotary inertia is to be neglected, then terms containing ρI must be set equal to zero (but not ρIE). Using both these simplifications, one arrives at the simpler Euler-Bernoulli equation. With non-dimensional parameters from Table 1:

$$W^{IV} + [\nu + \mu^2\Omega^2 + \mu^2\Omega^2\gamma]W'' + [\mu^4\Omega^4 - \Omega^2]W = 0 \quad \text{or} \quad W^{IV} + fW'' + gW = 0 \tag{8}$$

The following is the characteristic equation:

$$\lambda^4 + f\lambda^2 + g = 0 \quad \text{or} \quad \tilde{z}^2 + f\tilde{z} + g = 0 \quad \text{with} \quad \lambda^2 = \tilde{z} \tag{9}$$

The roots are then:

$$\tilde{z}_{1,2} = \frac{-f \pm \sqrt{f^2 - 4g}}{2} = \frac{1}{2}\left(-f \pm \sqrt{\Delta}\right) \quad \text{with} \quad \Delta = \nu^2 + \Omega^2(2\nu\mu^2 + 4) + \Omega^4[\mu^2(\mu^2 + 2\gamma\mu^2 + \gamma^2\mu^2 - 4\gamma)] \tag{10}$$

Carrying out a discussion about the signs of the roots $\tilde{z}_1$ and $\tilde{z}_2$ as a function of the natural frequency is necessary. $\tilde{z}_2 < 0$ for all values, while $\tilde{z}_1 > 0$ if $\sqrt{f^2 - 4g} > f \rightarrow g < 0 \rightarrow g = \Omega^2(\Omega^2\mu^4\gamma - 1) < 0 \rightarrow \Omega < \sqrt{\mu^{-4}\gamma^{-1}}$. On the other hand, $\tilde{z}_1 < 0$ if $\Omega > \sqrt{\mu^{-4}\gamma^{-1}}$. Note that this value is the cut-off frequency of the Timoshenko beam ([18] and [19]).

$$\Omega_{\text{co}} = \sqrt{\frac{1}{\mu^4\gamma}} \rightarrow \omega_{co} = c_0\Omega_{co} = \sqrt{\frac{EI}{\rho AL^4}}\sqrt{\frac{L^4GkA^2}{\rho I}} = \sqrt{\frac{GkA}{\rho I}} \tag{11}$$

The high frequencies $\Omega > \Omega_{co}$ represent the so called second spectrum of the Timoshenko beam, and as discussed in [17]–[19], have no physical meaning and should be disregarded. Therefore, the important case here is when $\tilde{z}_1 > 0$ and $\Omega < \Omega_{co}$. In this case the solution is found in the form:

$$W(\xi) = P_1\cosh(\lambda_1\xi) + P_2\sinh(\lambda_1\xi) + P_3\cos(\lambda_2\xi) + P_4\sin(\lambda_2\xi) \tag{12}$$

$$\lambda_1^2 = |\tilde{z}_1| = \frac{-f + \sqrt{\Delta}}{2} \quad \text{and} \quad \lambda_2^2 = |\tilde{z}_2| = \frac{f + \sqrt{\Delta}}{2} \tag{13}$$

The constants P_i $(i = 1,2,3,4)$ are determined by the boundary conditions. At the bottom of the tower ($z = 0, \xi = 0$) the sum of shear forces (1) and bending moments (2) equal to zero, and at the top of the tower ($z = L, \xi = 1$) as well the sum of shear forces (3) and bending moments (4) equal to zero.

(1) $\boldsymbol{W'''(0) + [\nu + \eta_{LR} + \mu^2\Omega^2(1+\gamma)]W'(0) + \eta_L W(0) = 0}$ (2) $\boldsymbol{W''(0) - \eta_R W'(0) - \eta_{LR} W(0) = 0}$

(3) $W'''(1) + [\nu + \mu^2\Omega^2(1+\gamma)]W'(1) + \alpha\Omega^2 W(1) = 0$ (4) $W''(1) - \beta\Omega^2 W'(1) = 0$

Substituting the solution in Equation 35 into the boundary conditions, a transcendental equation is obtained for the natural frequency by setting the determinant of the matrix in Equation 37 to zero.:

$$\boldsymbol{M} = \begin{bmatrix} \eta_L & [\nu + \eta_{LR} + \mu^2\Omega^2(1+\gamma)]\lambda_1 + \lambda_1^3 \\ \lambda_1^2 - \eta_{LR} & -\eta_R\lambda_1 \\ [\lambda_1^3 + (\nu + \mu^2\Omega^2(1+\gamma))\lambda_1]\sinh(\lambda_1) + \alpha\Omega^2\cosh(\lambda_1) & [\lambda_1^3 + (\nu + \mu^2\Omega^2(1+\gamma))\lambda_1]\cosh(\lambda_1) + \alpha\Omega^2\sinh(\lambda_1) \\ \lambda_1^2\cosh(\lambda_1) - \beta\Omega^2\lambda_1\sinh(\lambda_1) & \lambda_1^2\sinh(\lambda_1) - \beta\Omega^2\lambda_1\cosh(\lambda_1) \end{bmatrix} \quad (14)$$

$$\begin{bmatrix} \eta_L & [\nu + \eta_{LR} + \mu^2\Omega^2(1+\gamma)]\lambda_2 - \lambda_2^3 \\ -\lambda_2^2 - \eta_{LR} & -\eta_R\lambda_2 \\ [\lambda_2^3 - (\nu + \mu^2\Omega^2(1+\gamma))\lambda_2]\sin(\lambda_2) + \alpha\Omega^2\cos(\lambda_2) & [-\lambda_2^3 + (\nu + \mu^2\Omega^2(1+\gamma))\lambda_2]\cos(\lambda_2) + \alpha\Omega^2\sin(\lambda_2) \\ -\lambda_2^2\cos(\lambda_2) + \beta\Omega^2\lambda_2\sin(\lambda_2) & -\lambda_2^2\sin(\lambda_2) - \beta\Omega^2\lambda_2\cos(\lambda_2) \end{bmatrix}$$

The non-dimensional numbers are calculated for several real world wind turbines as presented in [9], [10], and the results calculated by present method are shown in Table 3-5.

3. Discussion of results

3.1 Frequency results

Non-dimensional numbers were determined for four offshore wind turbines for which the measured and/or estimated natural frequencies are available in the literature ([14], [16], [9]). The information necessary for frequency estimation are given in Table 2, the non-dimensional variables are calculated in Table 3 and the results of the proposed model along with comparison is given in Table 4. The approximations tend to underestimate the natural frequency except for the Lely A2 wind farm. It is to be noted here that the model uses a constant average thickness for the towers determined based on the range of thickness available in the literature and the masses of the towers. Real towers tend to have thicker walls in the bottom section and thinner ones in the upper sections, which increases the tower's natural frequency as compared to a constant thickness. As the natural frequency was found to be highly sensitive to the chosen wall thickness, this parameter may be the reason behind the underestimation. There are many other sources of uncertainty, including but not limited to damping of the whole system (soil, structural, aerodynamic, hydrodynamic), lengths of the components, soil parameters and foundation stiffness, flexibility of support structure connections and mass moment of inertia.

3.2 Natural frequency vs foundation stiffness curves

One of the aims of this analysis is to study the effect of change of soil parameters during the operation of the turbine i.e. how much the frequency will change if soil softens or stiffens due to repeated cyclic loading. This change in foundation stiffness has been reported [7] and change in the natural frequency of a wind turbine was also observed in [4] and also in case of the Hornsea Met Mast Twisted Jacket foundation [8]. However, the analysis is also useful to predict the effect of inaccurate estimation of foundation stiffness. The studied wind turbines are placed on relative frequency curves based on their estimated foundation stiffness values. The relative frequency shown on the ordinates is the ratio of the first natural frequency of the OWT structure and the natural frequency estimated by taking a fixed base, that is, $f_r = f/f_{FB}$. Fig 2 plots the relationship between two non-dimensional support stiffness (η_L and η_R) and the relative frequency for various values of cross-coupling stiffness (K_{LR}). It can be concluded from these graphs that with the increase of the cross-spring stiffness the OWT is closer to the high-slope zone of the curves. In such circumstances, the changes in the stiffness parameters introduces a higher change in natural frequency. In Figure 3, several wind turbines are placed in the relative frequency figures with respect to the three stiffness parameters. Each line style shows the relative frequency curve of a given OWT, and the estimated values on the curves are also shown for each turbine. In general, the sensitivity of the natural frequency to each parameter may be characterised by the slope of the curve at the estimated stiffness values.

3.3 A few design pointers may be deduced:

(a) From a design point of view it is important to note that the non-dimensional stiffness values have a certain region where the frequency function becomes flat i.e. any change in foundation stiffness will have very little impact on the natural frequency. The designer may wish to choose combination of tower stiffness (EI) and foundation stiffness (K_L, K_R and K_{LR}) such as to remain in the safe region to ensure that even if the stiffness parameters change during the lifetime of the turbine, the natural frequency will not be affected greatly.

(b) It can be observed that the structures are relatively insensitive to the lateral stiffness (K_L) and the most important factor is the rotational stiffness (K_R). In general, one can conclude that the change in rotational stiffness of the foundation causes the greatest change in natural frequency.

(c) The cross stiffness (K_{LR}) also has important effects and may not be neglected.

4. Conclusions

An analytical method is presented to predict the natural frequency of an offshore wind turbine where the tower is modelled as a beam and the foundation is idealised by three coupled springs. Two types of beam models (Timoshenko

and Euler Bernoulli) have been used to derive an equation for the natural frequency analytically Pysically meaningful non-dimensional groups have been formulated, which are particularly useful to study the problem at different scales (laboratory size scaled models and different prototype turbines). Typical values of these non-dimensional groups are calculated for several wind turbines and their natural frequency are predicted and compared (where possible). It was observed that the results produced by the proposed method give reasonably accurate initial estimates of the natural frequency of the structures. Comparison between the Euler-Bernoulli and the Timoshenko beam models reveals that the relatively complex Timoshenko beam theory does not improve the accuracy of the natural frequency prediction.

Table 2 – Input information, non-dimensional numbers, and natural frequency results for several turbines

Wind turbine	Lely A2: NM41 2-bladed	North Hoyle Vestas V80 2MW	Irene Vorrink 600kW	Walney 1 Siemens 3.6MW
Given and calculated geometric and material data				
Equivalent bending stiffness - EI [GNm]	22	133	21.5	274
Young's modulus of the tower material - E [GPa]	210	210	210	210
Shear modulus of the tower material - G [GPa]	79.3	79.3	79.3	79.3
Tower height - L [m]	41.5	70	51	83.5
Bottom diameter - D_b [m]	3.2	4.0	3.5	5.0
Top diameter - D_t [m]	1.9	2.3	1.7	3.0
Tower wall thickness range - t [mm]	~12	~35	8..14	20..80
Lateral foundation stiffness - K_L[GN/m]	0.83	3.1..3.5	0.76	3.65
Rotational foundation stiffness - K_R [GNm/rad]	20.6	33.8..62.1	15.5	254.3
Cross-coupling foundation stiffness - K_{LR} [GN]	-2.22	-1.71	-2.35	-20.1
Top mass (rotor-nacelle assembly) - M_2[kg]	32 000	100 000	35 700	234 500
Tower mass - M_3 [kg]	31 440	130 000	31 200	260 000
Average wall thickness - t_h [mm]	12	35	11	40
Shear coefficient - k [-]	0.5328	0.5328	0.5326	0.5327
Non-dimensional parameters				
Non-dimensional lateral stiffness - η_L	2698	11775	5880	7763
Non-dimensional rotational stiffness - η_R	38.88	28	39.64	77.49
Non-dimensional cross-coupling stiffness - η_{LR}	-174	-63	-284	-511.7
Non-dimensional axial force – ν	0.033	0.011	0.030	0.043
Mass ratio – α	1.018	0.760	1.144	0.9
Non-dimensional rotary inertia – β	0	0	0	0
Frequency scaling parameter - c_0	3.130	1.323	2.035	1.3454
Non-dimensional radius of gyration - μ	0.0214	0.0161	0.01795	0.0168
Non-dimensional shear parameter - γ	4.970	4.970	4.970	4.97
Natural frequency results				
Measured value - f_m[Hz]	0.634	N/A	0.546	0.35
Result produced by [9] - f_S [Hz]	0.740	0.345	0.457	-
Present study (Euler-Bernoulli) - f_{E-B} [Hz] (error [%])	0.735 (15.9%)	0.345 (N/A)	0.456 (16.5%)	0.331(5.9%)
Present study (Timoshenko) - f_T [Hz] (error[%])	0.734 (15.8%)	0.345 (N/A)	0.456(16.5%)	0.331(5.9%)
Fixed Base frequency (infinitely stiff foundation)	0.765	0.364	0.475	0.345

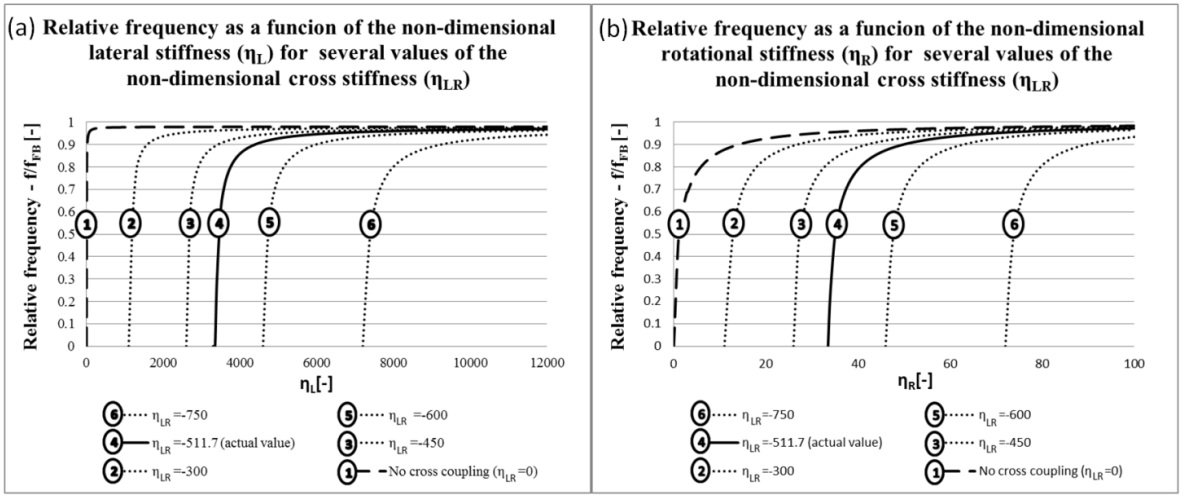

Figure 2 –Relative frequency as a function of (a) the non-dimensional lateral stiffness, (b) the non-dimensional rotational stiffness for several values of the non-dimensional cross stiffness.

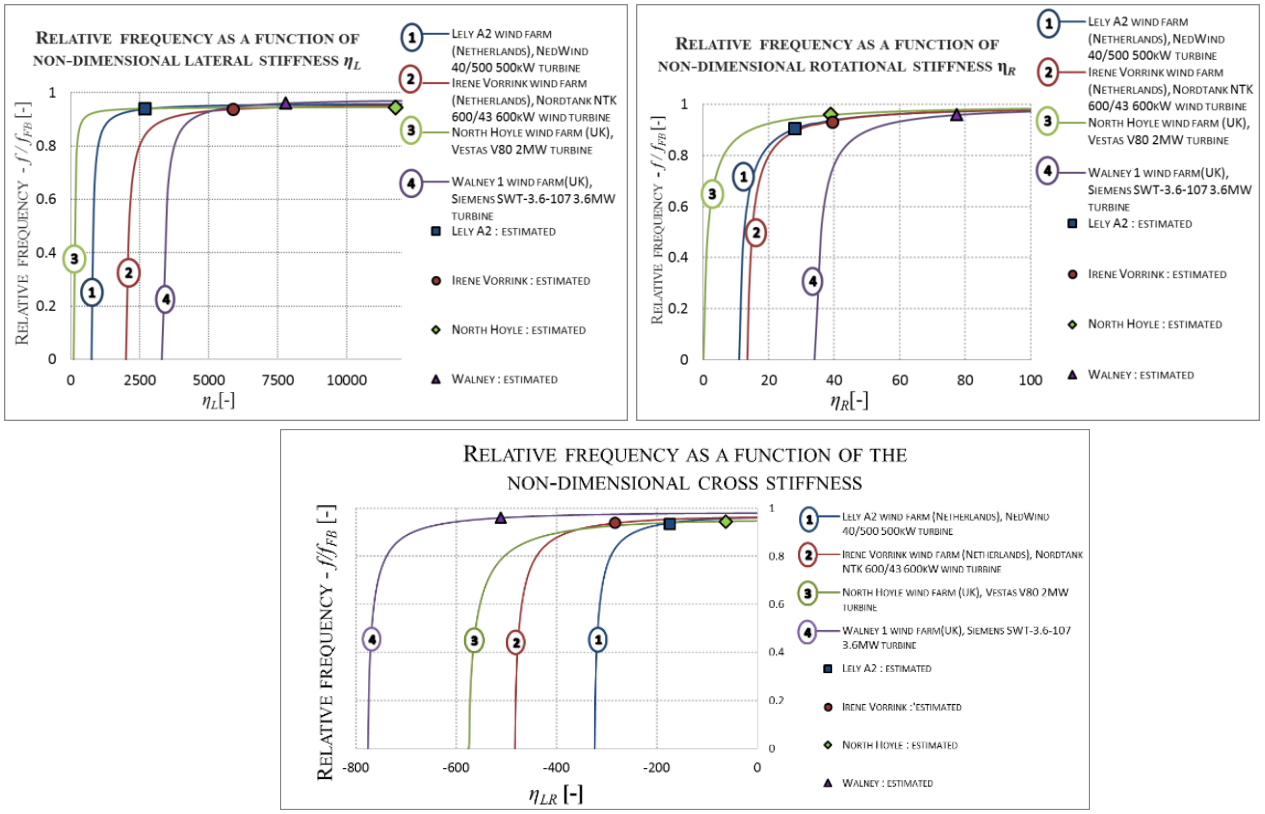

Figure 3 – Relative frequency as a function of the non-dimensional stiffness

References:

[1] S. Bhattacharya, D. Lombardi, and D. Muir Wood, "Similitude relationships for physical modelling of monopile-supported offshore wind turbines," *Int. J. Phys. Model. Geotech.*, vol. 11, no. 2, pp. 58–68, Jun. 2011.

[2] S. Bhattacharya, N. Nikitas, J. Garnsey, N. A. Alexander, J. Cox, D. Lombardi, D. Muir Wood, and D. F. T. Nash, "Observed dynamic soil – structure interaction in scale testing of offshore wind turbine foundations," *Soil Dyn. Earthq. Eng.*, 2013.

[3] S. Bhattacharya, J. a. Cox, D. Lombardi, and D. M. Wood Muir Wood, "Dynamics of offshore wind turbines supported on two foundations," *Proc. ICE - Geotech. Eng.*, vol. 166, no. 2, pp. 159–169, Apr. 2013.

[4] M. Kühn, "Soft or stiff: A fundamental question for designers of offshore wind energy converters," in *Proc. European Wind Energy Conference EWEC '97*, 1997.

[5] J. van der Tempel and D. Molenaar, "Wind turbine structural dynamics-a review of the principles for modern power generation, onshore and offshore," *Wind Eng.*, vol. 26, no. 4, pp. 211–220, 2002.

[6] S. Bhattacharya and S. Adhikari, "Experimental validation of soil–structure interaction of offshore wind turbines," *Soil Dyn. Earthq. Eng.*, vol. 31, no. 5–6, pp. 805–816, May 2011.

[7] D. Lombardi, S. Bhattacharya, and D. Muir Wood, "Dynamic soil–structure interaction of monopile supported wind turbines in cohesive soil," *Soil Dyn. Earthq. Eng.*, vol. 49, pp. 165–180, Jun. 2013.

[8] J. Lowe, "Hornsea Met Mast - A Demonstration of the 'Twisted Jacket' Design," *Power Point Presentation*, 2012. .

[9] S. Adhikari and S. Bhattacharya, "Vibrations of wind-turbines considering soil-structure interaction," *Wind Struct.*, vol. 14, no. 2, pp. 85–112, 2011.

[10] S. Adhikari and S. Bhattacharya, "Dynamic analysis of wind turbine towers on flexible foundations," *Shock Vib.*, vol. 19, no. 1, pp. 37–56, 2012.

[11] S. P. Timoshenko, "On the correction for shear of the differential equation for transverse vibrations of prismatic bars," *Philos. Mag.*, vol. 41, pp. 744–746, 1921.

[12] S. P. Timoshenko, "On the transverse vibrations of bars of uniform cross-section," *Philos. Mag.*, vol. 43, no. 253, pp. 125–131, 1922.

[13] S. Bhattacharya, "SDOWT: USER MANUAL (Simplified Dynamics of Wind Turbines)," Bristol, 2011.

[14] G. Gazetas, "Seismic response of end-bearing single piles," *Int. J. Soil Dyn. Earthq. Eng.*, vol. 3, no. 2, pp. 82–93, Apr. 1984.

[15] European Committee for Standardization, "Eurocode 8: Design of Structures for earthquake resistance - Part 5: Foundations, retaining structures and geotechnical aspects," 2003.

[16] K. Lesny, S. Paikowsky, and A. Gurbuz, "Scale effects in lateral load response of large diameter monopiles," *Geotech. Spec. Publ.*, no. 158, 2007.

[17] L. Majkut, "Free and forced vibrations of timoshenko beams described by single difference equation," *J. Theor. Appl. Mech.*, vol. 47, no. 1, pp. 193–210, 2009.

[18] N. G. Stephen and S. Puchegger, "On the valid frequency range of Timoshenko beam theory," *J. Sound Vib.*, vol. 297, no. 3–5, pp. 1082–1087, Nov. 2006.

[19] N. G. Stephen, "The second spectrum of Timoshenko beam theory—Further assessment," *J. Sound Vib.*, vol. 292, no. 1–2, pp. 372–389, Apr. 2006.